

# Anthropogenic Emissions of Hydrogen Chloride and Fine Particulate Chloride in China

Xiao Fu,<sup>\*,†</sup> Tao Wang,<sup>\*,†</sup> Shuxiao Wang,<sup>‡,§</sup> Lei Zhang,<sup>||</sup> Siyi Cai,<sup>‡</sup> Jia Xing,<sup>‡</sup> and Jiming Hao<sup>‡,⊥</sup>

<sup>†</sup>Department of Civil and Environmental Engineering, Hong Kong Polytechnic University, Hong Kong 99907, China

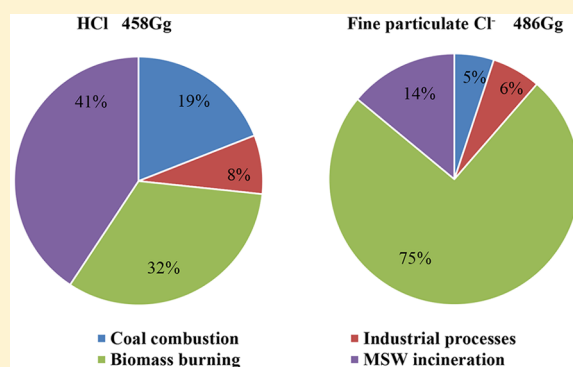
<sup>‡</sup>State Key Joint Laboratory of Environmental Simulation and Pollution Control, School of Environment, and <sup>⊥</sup>Collaborative Innovation Center for Regional Environmental Quality, Tsinghua University, Beijing 100084, China

<sup>§</sup>State Environmental Protection Key Laboratory of Sources and Control of Air Pollution Complex, Beijing 100084, China

<sup>||</sup>School of the Environment, Nanjing University, 163 Xianlin Avenue, Nanjing, Jiangsu 210023, China

## Supporting Information

**ABSTRACT:** Particulate chloride ( $\text{Cl}^-$ ) can be transformed to nitril chloride ( $\text{ClNO}_2$ ) via heterogeneous reaction with nitrogen pentoxide ( $\text{N}_2\text{O}_5$ ) at night. Photolysis of  $\text{ClNO}_2$  and subsequent reactions of chlorine radical with other gases can significantly affect the atmospheric photochemistry. In China, the only available integrated anthropogenic chloride emission inventory was compiled in the 1990s with low spatial resolution, which hinders assessment of impact of  $\text{ClNO}_2$  on current air quality. In this study, we developed an up-to-date and high-resolution anthropogenic inventory of hydrogen chloride (HCl) and fine particulate  $\text{Cl}^-$  emissions in China for 2014 with  $0.1^\circ \times 0.1^\circ$  resolution. Detailed local data and county-level activity data were collected and compiled. The anthropogenic emissions of HCl and fine particulate  $\text{Cl}^-$  in 2014 were estimated to be 458 and 486 Gg, respectively. Biomass burning was the largest contributor, accounting for 75% of fine particulate  $\text{Cl}^-$  emission and 32% of HCl emission. Northeast China and North China Plain were the largest chloride emitters. The monthly distribution varied in different regions, due to different agricultural activities and climate conditions. This work updates the chloride emission information and improves its spatial and temporal resolution, which enables better quantification of the  $\text{ClNO}_2$  production and its impact over China.



## 1. INTRODUCTION

Chlorine atom ( $\text{Cl}\cdot$ ) plays important roles in atmospheric chemistry, including depleting ozone and oxidizing methane, other hydrocarbons, and elemental mercury.<sup>1</sup> Particulate  $\text{Cl}^-$  has been identified as a crucial species for chlorine chemistry in the troposphere. It can be converted to nitril chloride ( $\text{ClNO}_2$ ) via heterogeneous reaction with nitrogen pentoxide ( $\text{N}_2\text{O}_5$ ),<sup>2</sup> and photolysis of  $\text{ClNO}_2$  releases chlorine atom which can react many organic gases<sup>3</sup> and can have considerable impact on ozone production.<sup>4,5</sup> A comprehensive assessment of the role of chlorine initiated reactions in atmospheric chemistry and air quality requires understanding the sources of chlorine, among which particulate  $\text{Cl}^-$  and gaseous hydrogen chloride (HCl) are the important ones.

Particulate  $\text{Cl}^-$  can be emitted directly or generated via equilibrium repartition of gaseous HCl. Ocean is the dominant natural emission source of particulate  $\text{Cl}^-$ , but observation studies have also demonstrated the importance of anthropogenic chloride emissions.<sup>3–5</sup> Global emission of anthropogenic inorganic chloride was 12 900 Gg in 1990 based on the Reactive Chlorine Emission Inventory (RCEI) developed by the International Global Atmospheric Chemistry Program's

Global Emissions Inventory Activity (GEIA).<sup>6</sup> Of the total inorganic chloride emissions, 49%, 36%, and 16% were from biomass burning, coal combustion, and waste incineration, respectively. The RCEI\_1990 data is the only available integrated anthropogenic chloride emission inventory for China. The total inorganic chloride emission in China was estimated to be 2225 Gg in 1990, of which 42%, 37%, and 21% were from biomass burning, coal combustion, and waste incineration, respectively. This emission inventory was compiled for the year 1990 and has not been updated since then. Given that the rapid economic and industrial development in China has resulted in significant changes in fuel consumptions and pollution control technologies in the last three decades, chloride emissions derived from the RCEI\_1990 data are outdated. In addition, most parameters adopted in RCEI\_1990, such as Cl content in coal and technology type, were not based on Chinese local investigations. Finally, the

Received: September 28, 2017

Revised: January 15, 2018

Accepted: January 17, 2018

Published: January 27, 2018

RCEI\_1990 was compiled with a coarse spatial resolution of  $1^\circ$  ( $\sim 100$  km), making it difficult to assess the impact of chlorine chemistry at a finer scale in China.

In this study, we developed an up-to-date anthropogenic inventory of gaseous HCl and fine particulate  $\text{Cl}^-$  emissions for the Chinese mainland (not including Hong Kong, Macao, and Taiwan) for the year 2014. Detailed Chinese local data (e.g., Cl content in coal, control technologies, point source information, etc.) and county-level activity data were collected and compiled. Sectoral, spatial, and temporal distributions of chloride emissions are presented in sections 3.1, 3.2, 3.3, respectively. Comparison with RCEI\_1990 and uncertainties and their major causes were also discussed.

## 2. MATERIALS AND METHODS

In this study, we grouped chloride emission sources into four major sectors, including coal combustion, industrial processes, biomass burning, and municipal solid waste (MSW) incineration. Each sector was divided into subsectors based on different technologies and processes, as shown in Table S1. An emission factor method was applied to estimate gaseous HCl and fine particulate  $\text{Cl}^-$  emissions, which was implemented by the following equations

$$E_{\text{HCl}} = \sum_{i,j} A_{i,j} \text{EF}_{(\text{HCl})i,j} \quad (1)$$

$$E_{\text{PM}_{2.5}\text{Cl}^-} = \sum_{i,j} (A_{i,j} \text{EF}_{(\text{PM}_{2.5})i,j}) M_j \quad (2)$$

where  $A$  is activity data, covering the amount of coal consumption, burned biomass and burned MSW, and the output of industrial products;  $\text{EF}_{\text{HCl}}$  and  $\text{EF}_{\text{PM}_{2.5}}$  are HCl and  $\text{PM}_{2.5}$  emission factors;  $M$  is the percentage of  $\text{Cl}^-$  in  $\text{PM}_{2.5}$  emission.  $i, j$  represent the county and subsectors, respectively.

In order to achieve a better spatial distribution, activity data were compiled at county level. Additionally, we established a new database for point sources, containing 2186 power plants, 735 cement plants using precalciner kilns, 345 iron and steel plants, and 171 municipal solid waste incineration plants, with detailed information on latitude/longitude location, installed capacity, production, technology, and pollution control facility.

**2.1. Activity Data.** **2.1.1. Coal Combustion and Industrial Processes.** Provincial coal consumptions for power plants, domestic combustion, and total industrial combustion were obtained from Chinese official energy statistics,<sup>7</sup> including raw coal, cleaned coal, and briquette coal. The industrial outputs were obtained from Chinese industrial statistics.<sup>8</sup> In the sector of industrial processes, the production of cement clinker, iron, lime, and brick also consumed coal. In order to avoid double counting, the coal consumptions by these industrial processes were subtracted from coal consumed by total industry, which were calculated as the products of industrial outputs and the corresponding coal intensities. The coal intensities for cement clinker production were estimated as 114, 126, and 163 kg coal equivalent (kce) per ton clinker for precalciner, shaft, and other rotary kilns, respectively.<sup>9</sup> For lime production, China Lime Association estimated a coal intensity of 145 kce/ton lime production.<sup>10</sup> For brick production, coal intensities of 800 kce/10 000 solid clay bricks and 200 kce/10 000 hollow bricks were applied.<sup>11</sup>

For power plants, provincial coal consumptions were distributed to each plant based on its installed capacity. For

industrial and domestic combustion, coal consumptions at county resolution were compiled based on industrial gross domestic product (GDP) and population at county resolution, respectively.<sup>12–14</sup>

**2.1.2. Biomass Burning.** For crop straw, the burning mass was calculated by the following equation

$$A_{i,j,k} = P_{i,j} \times R_j \times F_{i,j,k} \times D_j \times C_j \quad (3)$$

where  $A$  is burning mass of crop straw;  $P$  is crop yield;  $R$  is straw-to-product ratio;  $F$  is the fraction for different burning type (open burning and household burning);  $D$  is dry matter fraction;  $C$  is combustion efficiency.  $i, j,$  and  $k$  represent the county, crop type, and burning type, respectively. Crop yields at county level were compiled based on crop yields at province level<sup>8</sup> and crop sowing area at county level for each crop.<sup>15</sup> The provincial fractions of open burning and household burning were based on national investigations.<sup>16–18</sup> The  $R, D,$  and  $C$  values were obtained from the study of Zhou et al.,<sup>18</sup> which has reviewed and integrated a collection of literature.

For firewood burning, we obtained firewood consumption data before the year 2008<sup>19</sup> and in the year 2012.<sup>20</sup> Firewood consumption presented a linear declining trend during 2005–2012, and the average decreasing rate was 4.2 Mtce/year. Firewood consumption in the year 2014 was estimated based on its interannual variation trend. Firewood consumption data at county level were compiled based on provincial firewood consumption data and nonurban population at county level.<sup>12,14</sup>

For forest and grass burning, the burning mass of forest and grass was calculated by the following equation

$$A_{i,j} = \text{BA}_{i,j} \times \text{FL}_{i,j} \times \text{CF}_j \quad (4)$$

where  $A$  is burning mass of forest and grass;  $\text{BA}$  is the burned area;  $\text{FL}$  is biomass fuel loading;  $\text{CF}$  is combustion factor;  $i$  and  $j$  represent the county and land cover type. Burned areas at county level were compiled based on those at province level from statistic data,<sup>8</sup> and forest/grass distribution derived from the 500 m resolution MODIS Land Cover product (MCD12Q1). Seven vegetation types were considered as forest, including evergreen needle-leaf forest, evergreen broad-leaf forest, deciduous needle-leaf forest, deciduous broad-leaf forest, mixed forest, closed shrubland, and open shrubland. Three vegetation types were considered as grass, including woody savannas, savannas, and grassland. Provincial biomass fuel loading for different vegetation was gained from Chinese local research.<sup>18,21–23</sup> Combustion factor for different vegetation was obtained from the study of Zhou et al.<sup>18</sup>

**2.1.3. Municipal Solid Waste Incineration.** With the rapid economic and industrial development, great amounts of MSW have been produced in China. Incineration is a crucial technology for MSW treatment. Provincial amounts of MSW incineration were gathered from Chinese statistical data<sup>8</sup> and then distributed to each MSW incineration plant based on its MSW treatment capacity. In 2014, 53 300 Gg MSW were treated in MSW incineration plants, accounting for 32.5% of the total MSW with harmless treatment. Jiangsu, Zhejiang, and Guangdong are the provinces with greatest MSW incineration capacities.

In addition to MSW incineration treatment, MSW open burning also occurred frequently, especially in urban–rural conjunctions and rural regions. The mass of MSW burned by open burning was calculated by the following equation

$$W_i = (MSW_{urban,i} \times P_{urban,i} \times F_{urban,i} + MSW_{n-urban,i} \times P_{n-urban,i} \times F_{n-urban,i}) \times 365 \times B \quad (5)$$

where  $W$  is the mass of MSW burned;  $P_{urban}$  and  $P_{n-urban}$  are the population living in urban and nonurban (including suburban, town, and village) region, respectively;  $MSW_{urban}$  and  $MSW_{n-urban}$  are the mass of MSW production per capital per day for urban and nonurban region, respectively.  $F_{urban}$  and  $F_{n-urban}$  are the fractions of MSW burned by open burning.  $B$  is the burnable part in waste actually burned, and the IPCC recommended value of 0.6 was adopted.<sup>24</sup>

Urban and nonurban population at county level were obtained from Chinese statistic data.<sup>12,14</sup> Provincial  $MSW_{urban}$  values were derived from Wang et al.,<sup>25</sup> and the national average is 1.2 kg/capital/day. Regional values from He et al.<sup>26</sup> were used for  $MSW_{n-urban}$ , and the national average is 0.79 kg/capital/day.  $F_{urban}$  was estimated as the fraction of total MSW which was not treated. The treatment rates for urban area at city level can be obtained from Chinese statistic data.<sup>14</sup> In nonurban region, the regional treatment rates from He et al.<sup>26</sup> were used.

## 2.2. Emission Factors of HCl. 2.2.1. Coal Combustion.

HCl emission factor for coal combustion was calculated by the following equation

$$EF_{(HCl)ij,k} = C_i R_{j,k} \sum_l (1 - f_{(SO_2)ij,k,l} \eta_{(SO_2)ij,k,l}) \sum_m (1 - f_{(PM)ij,k,m} \eta_{(PM)ij,k,m}) \quad (6)$$

where  $C$  is the average Cl content in consumed coal;  $R$  is the HCl release rate;  $f_{(SO_2)}$  and  $f_{(PM)}$  are application rates of conventional  $SO_2$  and particulate matter (PM) emission control technologies, which were derived from the emission database established in our previous studies;<sup>27–29</sup>  $\eta_{(SO_2)}$  and  $\eta_{(PM)}$  are removal efficiencies of conventional  $SO_2$  and PM emission control technologies for HCl;  $i, j, k, l$ , and  $m$  represent the province, subsector, technology/fuel type,  $SO_2$  emission control technology, and PM emission control technology, respectively.

*a. Cl Content in Coal.* Coal resources are distributed very unevenly in China. As shown in Table 1, over 60% of coal was mined from Inner Mongolia, Shanxi and Shaanxi province. However, a large amount of coal was consumed in regions with developed economy and industry, like Shandong, Jiangsu, Hebei, and Guangdong province. In order to estimate the chloride emissions from coal combustion reliably, we calculated the Cl content in raw coal consumed by each province by the following equation:

$$C_{rc-consumed} = M_c C_{rc-produced} \quad (7)$$

where  $C_{rc-consumed}$  is the vector of Cl content in raw coal consumed by each province;  $C_{rc-produced}$  is the vector of Cl content in raw coal produced by each province;  $M_c$  is coal transportation matrix, which was compiled based on the methodology in Zhang et al.<sup>30</sup>

For Cl content in produced raw coal, a variety of measurement data was gathered, including the United States Geological Survey (USGS) database, the Tsinghua database, and other Chinese studies,<sup>30–41</sup> which have covered major coal basins in China. For provinces with sufficient coal samples, we built the distribution functions for Cl content in coal. As shown

**Table 1. Cl Content in Raw Coal As Produced and Consumed by Province in China, 2014**

	coal production (Mt)	coal consumption (Mt)	Cl content in produced raw coal (ppm)	Cl content in consumed raw coal (ppm)
Anhui	130.11	154.44	192	244
Beijing	4.57	17.27	581	336
Chongqing	38.84	59.86	339	317
Fujian	15.90	81.39	260	288
Gansu	47.53	68.93	144	213
Guangdong	0.00	171.70	260	282
Guangxi	6.15	66.60	260	238
Guizhou	185.08	135.38	229	229
Hainan	0.00	10.27	260	282
Hebei	73.45	294.22	581	336
Heilongjiang	70.59	133.54	245	175
Henan	144.15	232.23	333	313
Hubei	10.57	120.25	333	299
Hunan	55.53	110.25	260	274
Inner Mongolia	993.91	322.19	144	156
Jiangsu	20.19	269.32	192	258
Jiangxi	28.14	74.95	260	272
Jilin	31.00	103.98	245	190
Liaoning	50.01	169.44	204	176
Ningxia	85.63	85.67	298	294
Qinghai	18.33	17.26	260	185
Shaanxi	522.26	151.67	298	291
Shandong	146.84	390.14	332	290
Shanghai	0.00	46.54	192	214
Shanxi	927.94	328.47	287	248
Sichuan	76.63	108.49	339	329
Tianjin	0.00	49.58	581	336
Xinjiang	145.20	128.89	251	253
Xizang	0.00	0.00	260	245
Yunnan	47.41	87.40	212	260
Zhejiang	0.00	138.39	260	273

in Table S2, the median values of the Cl content in coal were significantly lower than the mean values, due to a long tail of the log-normal or skewed distributions. In this study, the median values were used in the case of the effects of a few high values. For provinces without sufficient coal samples, we used the median values of the calculated distribution curve from neighboring province or the national average distribution curve. The calculated Cl content in raw coal produced and consumed for each province is summarized in Table 1.

The Cl content of cleaned coal as produced was calculated by the following equation<sup>42</sup>

$$C_{cc-produced,i} = \frac{Q_{rc,i} C_{rc-consumed,i} (1 - \eta_{clean})}{P_{cc}} \quad (8)$$

where  $C_{cc-produced}$  is the Cl content in cleaned coal as produced;  $Q_{rc}$  is the amount of raw coal consumed for cleaned coal production;  $P_{cc}$  is the amount of cleaned coal production;  $\eta_{clean}$  is the fraction of Cl removed by the coal cleaning process, which was set as 70%<sup>43</sup> in this study;  $i$  is the province. The Cl content in cleaned coal as consumed was also calculated based on the coal transportation matrix.

The Cl content of briquette coal as produced was calculated by the following equation

$$C_{bc\text{-produced},i} = \frac{Q_{rc,i}C_{rc\text{-consumed},i} + Q_{cc,i}C_{cc\text{-consumed},i}}{P_{bc}} \quad (9)$$

where  $C_{bc\text{-produced}}$  is the Cl content in briquette coal as produced;  $Q_{rc}$  and  $Q_{cc}$  are the amounts of raw coal and cleaned coal consumed for briquette coal production;  $P_{bc}$  is the amount of briquette coal production;  $i$  is the province. The Cl content in briquette coal as consumed was also calculated based on the coal transportation matrix.

**b. HCl Release Rate.** The HCl release rates depend on combustion technologies. In this study, coal combustion facilities were divided into four types, including pulverized coal boiler, circulating fluidized bed boiler, stoker furnace, and stove. The proportions of each burning technology for power plants, industrial boilers, and domestic combustion were derived from the emission database established in our previous studies.<sup>27–29</sup> Based on the field measurements for six power plants in China,<sup>44</sup> the HCl release rate for pulverized coal boiler was set as 87%, ranging from 78% to 93%. Paradiz et al.<sup>45</sup> measured the HCl release rates of coal with different Cl contents in a stove, and the median value (68%) was employed as the HCl release rate for stove in this study. Due to lack of measurement results, the HCl release rates were set as 87% and 80% for circulating fluidized bed boiler and stoker furnace, respectively, referring to the  $SO_2$  release rates used in the previous studies.<sup>27–29</sup>

**c. HCl Emissions Control.** In order to improve air quality, power plants and industrial boilers have adopted a series of air pollution control devices. Field tests have demonstrated that these conventional air pollution control devices can also reduce HCl emissions. We reviewed and integrated the HCl removal efficiencies of different control devices (Table 2), and the average values were applied in this study.

**2.2.2. Other Sources.** HCl emission factors for other sources used in this study are listed in Table 3. For cement clinker production, sinter production, and MSW incineration, the HCl emission factors were derived from the field testing results of Chinese factories.<sup>51–54,58</sup> For biomass burning, MSW open burning, and HCl production, foreign testing results<sup>55–57,59–61</sup> were used. Because of the lack of the studies about HCl emissions from lime and brick production, the HCl emission factors in these two sources were calculated based on their coal consumption, using the same method for coal combustion.

**2.3. Cl<sup>-</sup> Percentages in Fine Particle Emissions.** The methodology for calculating  $PM_{2.5}$  emissions has been described in detail in the previous studies.<sup>18,27–29,60</sup> In this study, we focused on the Cl<sup>-</sup> percentages in  $PM_{2.5}$  emissions from different sources in order to estimate the fine particulate Cl<sup>-</sup> emissions. Table 4 summarizes the values used in this study, and the detail data are listed in Table S3. For most sources, the Cl<sup>-</sup> percentages were derived from Chinese local testing. Because no significant differences can be identified for different control devices, we did not consider their effects on Cl<sup>-</sup> percentages in  $PM_{2.5}$  emissions. Similarly, the testing results for biomass household and open burning were also combined. For lime kilns, MSW incineration, and forest/grass wild fires, the values from U.S. database<sup>62</sup> were used, due to lack of local testing data.

### 3. RESULTS AND DISCUSSION

#### 3.1. HCl and Fine Particulate Cl<sup>-</sup> Emissions by Sectors.

In 2014, the total emissions of HCl and fine particulate Cl<sup>-</sup> were 458 and 486 Gg, respectively. As shown in Figure 1, MSW

**Table 2. HCl Removal Efficiencies for Different Control Devices**

control device <sup>a</sup>	removal efficiency (%)	ref
WFGD	94.5	ref 44
WFGD	93.0	ref 44
WFGD	97.8	ref 44
WFGD	95.7	ref 44
WFGD	95.2	ref 44
WFGD	96.8	ref 44
WFGD	99.4	ref 46
WFGD	96.7	ref 47
WFGD	99.3	ref 47
WFGD	98.5	ref 47
WFGD	95.0	ref 48
other-FGD	94.0	ref 49
other-FGD	85.0	ref 50
other-FGD	90.0	ref 50
FF	9.5	ref 44
FF	11.3	ref 44
ESP	2.2	ref 44
ESP	6.4	ref 44
ESP	6.5	ref 44
ESP	3.4	ref 44
ESP	12.0	ref 46
ESP	0.9	ref 48
wet scrubber	50	ref 49
	In This Study	
WFGD	96.5	average
other-FGD	89.7	average
FF	10.4	average
ESP	5.2	average
wet scrubber	50	average

<sup>a</sup>WFGD: wet flue gas desulfurization. FF: fabric filter. ESP: electrostatic precipitator.

incineration was the largest contributor for HCl emissions, with a proportion of 41%. MSW open burning contributed approximately 98% to the total HCl emission from MSW incineration, although the mass of MSW burned just accounted for 46%. As shown in Table 3, the HCl emission factor of MSW open burning was much higher than that of MSW incineration plants because the MSW incinerators in China have all been equipped with advanced air pollution control devices (semidry scrubber with slaked lime slurry injection + activated carbon injection + fabric filter), which can reduce HCl emissions significantly. For MSW open burning, the masses of MSW burned in urban and nonurban region were comparative, with the proportion of 54% and 46%, respectively. Although more MSW was generated in urban region due to higher population density and more developed economy, more attention has been paid to MSW treatment. From 2005 to 2014, the amount of MSW with harmless treatment has doubled in urban region. In contrast, the MSW treatment in nonurban region was backward and needs to be improved in the future. Biomass burning was the second largest emission contributor, accounting for 32%. Coal combustion contributed about 19% for the total HCl emissions, of which power plants, industrial boilers, and domestic combustion contributed 33%, 35%, and 32%, respectively. Even though power plants consumed over 85% of coal, they did not contribute large HCl emissions due to advanced pollution control devices. Over 98% of power plants have been equipped with FGD in 2014. In the industrial

**Table 3. HCl Emission Factors for Industrial Processes, Biomass Burning, and MSW Incineration**

source category	emission factor	ref
cement kiln (g/t)	16.3	refs 51, 52, 53
sinter production (g/t)	0.6	ref 54
lime kiln (g/t)	29.72	calculated based on coal consumption
brick kiln (g/t)	2.57	calculated based on coal consumption
biomass burning—rice straw (g/kg)	0.44	ref 55
biomass burning—wheat straw (g/kg)	0.6	ref 55
biomass burning—sugar cane straw (g/kg)	0.1	ref 55
biomass burning—other crop straw (g/kg)	0.38	average of values for rice, wheat, and sugar cane straw
biomass burning—forest wild fire (g/kg)	0.41	ref 55
biomass burning—grass wild fire (g/kg)	0.06	ref 55
biomass burning—firewood (g/kg)	0.06	refs 55, 56, 57
MSW incineration plants—grated firing incinerator (g/kg)	0.2	ref 58
MSW incineration plants—fluidized bed incinerator (g/kg)	0.9	ref 58
MSW open burning (g/kg)	3.58	refs 56, 59, 60
HCl production (g/kg)	0.08	ref 61

**Table 4. Cl<sup>-</sup> Percentage in PM<sub>2.5</sub> Emission**

sector	Cl percentage in PM <sub>2.5</sub> emission (%)
pulverized coal boiler	1.10
circulating fluidized bed boiler	0.70
stoker furnace	2.77
stove	0.82
sinter production	5.60
puddling	3.54
cement kiln	0.73
lime kiln	1.53
brick kiln	0.82 <sup>a</sup>
biomass burning—wheat	9.75
biomass burning—corn	13.97
biomass burning—rice	14.80
biomass burning—rape	13.51
biomass burning—soybean	8.35
biomass burning—cotton	0.84
biomass burning—sorghum	1.63
biomass burning—other crop	8.98 <sup>a</sup>
biomass burning—forest/grass wild fires	4.15
biomass burning—firewood	2.75
MSW incineration	13.80

<sup>a</sup>The value for brick kiln was set as the same as that for stove, due to lack of testing data. The value for the other crop was set as the average value of the other seven crops with measurements.

processes sector, cement plants were the major emission source.

For fine particulate Cl<sup>-</sup> emissions, biomass burning contributed approximately 75% of the total emissions due to large PM<sub>2.5</sub> emissions and high Cl<sup>-</sup> percentages in PM<sub>2.5</sub> emissions, of which biomass household burning and open

burning accounted for 48% and 52%. MSW incineration was the second largest contributor, with a proportion of 14%. Industrial process contributed about 6% for the total fine particulate Cl<sup>-</sup> emissions, of which iron and steel plants accounted for about 58%, due to relative higher Cl<sup>-</sup> percentages in PM<sub>2.5</sub> emissions.

**3.2. Spatial Distribution of HCl and Fine Particulate Cl<sup>-</sup> Emissions.** Figure 2 shows the provincial HCl and fine particulate Cl<sup>-</sup> emissions. For HCl emissions, Heilongjiang, Henan, Shandong, Hebei, and Sichuan were the top five emitters, accounting for 7.5%, 7.2%, 7.0%, 6.4%, and 5.8% of the total HCl emissions, respectively. HCl emissions from MSW incineration were dominant for most provinces, except some large agricultural provinces, like Heilongjiang, Shandong, and Anhui, where the emissions from biomass burning were larger. For fine particulate Cl<sup>-</sup>, the top five emitters were Heilongjiang, Jilin, Henan, Shandong, and Inner Mongolia, which are all the major agricultural regions with high crop outputs in China, accounting for 12.9%, 7.4%, 6.9%, 6.8%, and 6.3% of the total emissions, respectively. For each sector, the provincial distribution was not the same. For MSW burning, Hebei was the province with the largest chloride emissions, where population density is high and MSW treatment needs to be improved. In the urban region of Shijiazhuang, the capital of Hebei province, the MSW treatment rate was just 74.68% in the year 2014. For biomass burning, the largest emission contributor was Heilongjiang, which is a major agricultural province, producing approximately 15.5% of corn and 10.9% of rice in China. Additionally, over 70% of crop straw was burned in Heilongjiang based on the investigation.<sup>16–18</sup> For coal burning and industrial process, Shandong was the largest contributor, which consumed approximately 9.2% of the total raw coal in China.

Figure 3 presents the spatial distribution of HCl and fine particulate Cl<sup>-</sup> emissions at a resolution of 0.1° × 0.1°. The emissions have been calculated at county level and then allocated into each grid based on various spatial information. The emissions from point sources were allocated to the corresponding grids based on their latitude/longitude coordinates. The emissions from biomass open burning and forest/grass wild fires were gridded using the method in Huang et al.<sup>63</sup> based on the MODIS active fire products (MOD14/MYD14) of 2010–2017. For other sources, the emissions were allocated into each grid based on population distribution. It can be seen that HCl and fine particulate Cl<sup>-</sup> emissions presented similar spatial patterns, which concentrated on the North China Plain, Northeast China, and Sichuan Basin. In these regions, NO<sub>x</sub> and particle concentrations are also high, so the ClNO<sub>2</sub> chemistry there would be significant and need more attention.

**3.3. Temporal Distribution of Chloride Emissions.** Figure 4 presented the monthly distribution of chloride emission (HCl + Cl<sup>-</sup>) in different regions. For biomass open burning and wild fires, the temporal variability was calculated based on the MODIS active fire products (MOD14/MYD14) of 2010–2017. The monthly variation of domestic coal combustion and household biomass burning was derived from Wang et al.,<sup>64</sup> which assumed the activity of stove operation depended on the provincial monthly mean temperature. For power plants, industry, and MSW incineration, we assumed that the monthly emission distribution was uniform. For biomass open burning, March, April, June, and October were the top four months with high emissions, corresponding to the major sowing and harvest times in China. For domestic

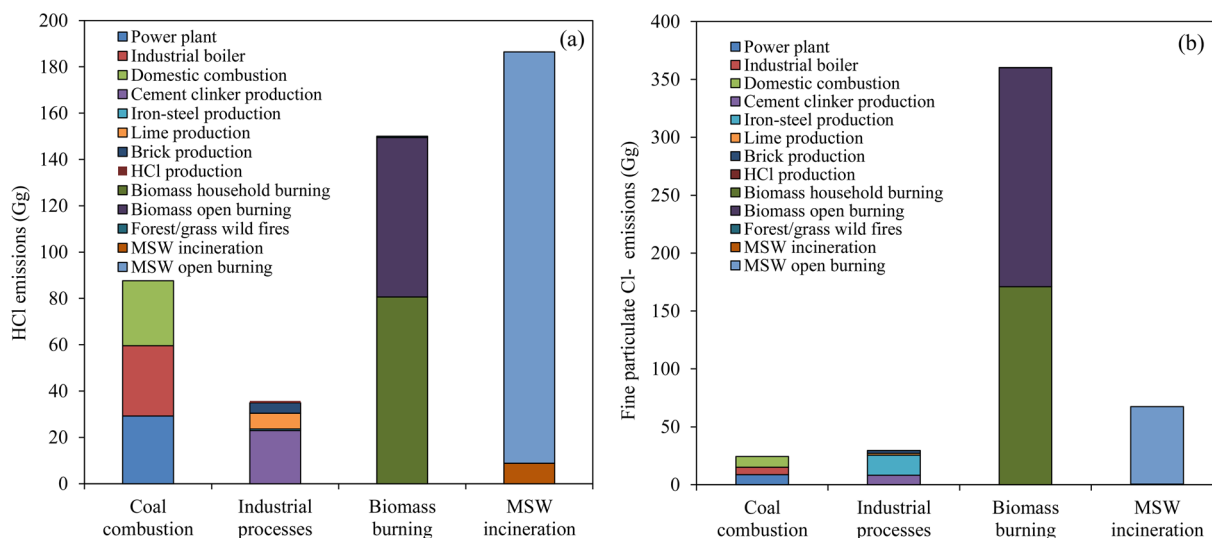


Figure 1. (a) HCl and (b) fine particulate Cl<sup>-</sup> emissions by sector.

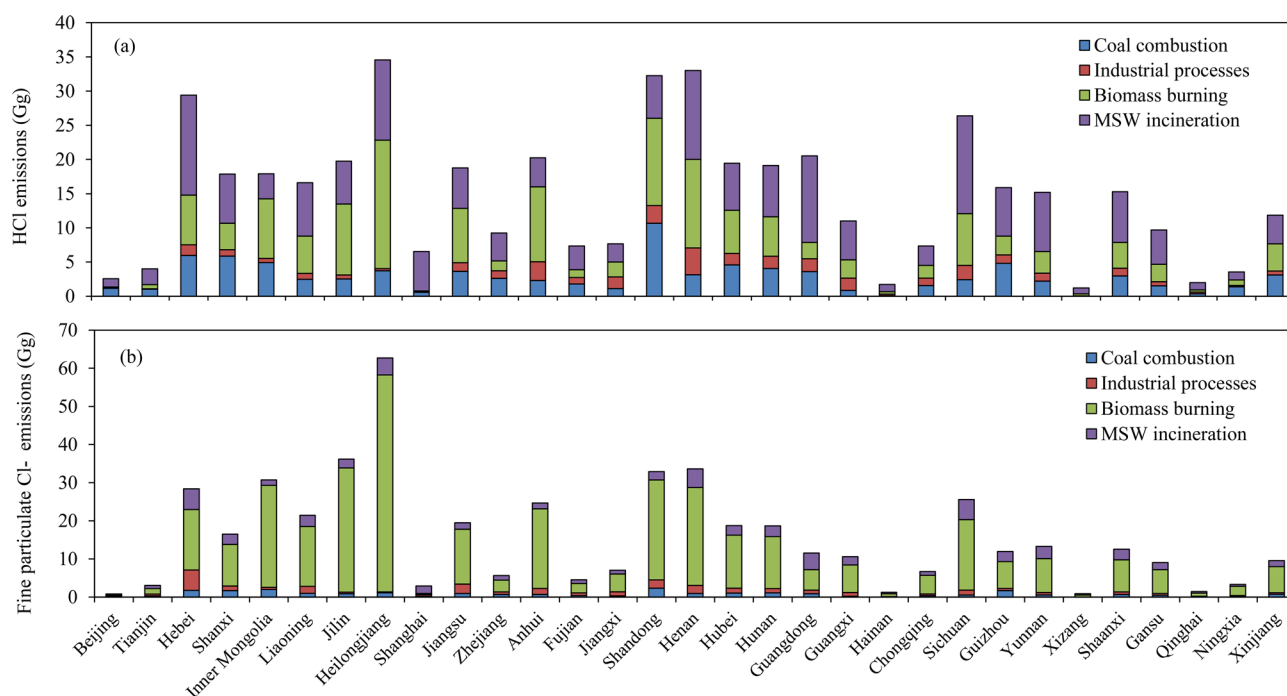
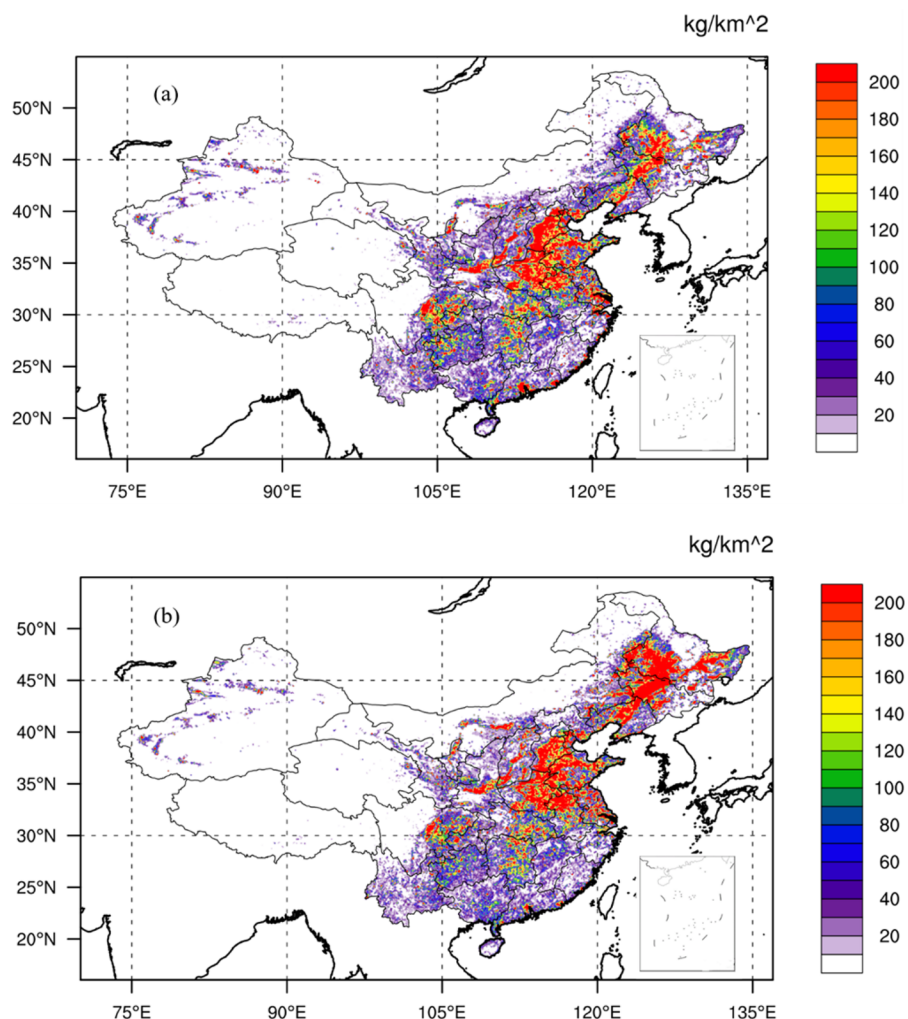


Figure 2. (a) HCl and (b) fine particulate Cl<sup>-</sup> emissions by province.

coal and household biomass burning, emissions were higher in cold season than in warm season due to heating activities. The monthly distributions in different regions were distinctly different. For example, in Northeast China (including Liaoning, Jilin, and Heilongjiang provinces), high emissions occurred in October, November, March, and April. The peak in October and November was due to the harvesting of rice and corn, and the peak in March and April was due to the sowing of rice and corn. In South China, the temporal distribution was more uniform than that in other regions, due to the warm climate condition all year around.

**3.4. Comparing with the RCEI\_1990.** Figure 5 presents the comparison of the total inorganic chloride (HCl + fine particulate Cl<sup>-</sup>) emissions between RCEI\_1990 and this study. It can be seen that the total inorganic chloride emission in RCEI\_1990 was approximately twice that of the 2014 value in

this study. For coal combustion and industrial sector, the inorganic chloride emission in RCEI\_1990 was approximately four times higher than that in this study. Although coal consumption had a fourfold increase from 1990 to 2014, many air pollution control devices were installed, leading to large chlorine removal. For example, the total chloride emission from power plants has been reduced by approximately 95% with air pollution control devices in 2014. For biomass burning, RCEI\_1990 estimated the chloride emission based on its relativity with the emitted amount of CO<sub>2</sub>, CO, or volatilized carbon. Different calculating method used in these two emission inventories may result in the differences of estimated chloride emissions. For MSW waste, the MSW generation in 2014 is larger than that in 1990, due to the growth of population and economy. However, the proportion of MSW treatment was higher in 2014. On the whole, the chloride



**Figure 3.** (a) HCl and (b) fine particulate  $\text{Cl}^-$  emissions distribution at  $0.1^\circ \times 0.1^\circ$  resolution.

emission from MSW burning in this study was lower than that in RCEI\_1990. Due to emission control efforts for coal combustion and waste burning in the past 20 years, the relative contribution from biomass burning (54%) is higher than that in 1990 (42%), suggesting that more attention should be paid to reducing biomass burning in the future for chloride emission control.

RCEI\_1990 was established 20 years ago and focused on the global scale. The present study updates and improves the chloride emissions in China in two ways. First, the new emission inventory made use of more detailed and finer localized data on emission factors and activities. Second, it provided the temporal variation and higher spatial resolutions of  $0.1^\circ \times 0.1^\circ$ . In comparison, RCEI\_1990 gave the annual total emissions at a resolution of  $1^\circ \times 1^\circ$ . Figure S1 presents the spatial distributions of chloride emissions ( $\text{HCl} + \text{Cl}^-$ ) in RCEI\_1990 data and this study. In order to compare the spatial distributions more clearly, the total chloride emission from RCEI\_1990 data presented in Figure S1 has been adjusted to be equal to the total chloride emission in this study. It can be seen that differences existed for spatial distribution of chloride emissions in RCEI\_1990 data and this study. For the sectors of coal combustion, industrial processes, and waste incineration, the spatial distribution patterns of these two emission inventories were similar, but the regions with high chloride

emission intensities were more concentrated in this study than RCEI\_1990, due to finer spatial resolution. For biomass burning sector, the chloride emission in Northeast China was much lower than that in North China Plain based on RCEI\_1990 data. However, the chloride emissions from biomass burning in these two regions were comparative in this study. Northeast China is one of the most important agricultural regions, and meanwhile, high percentage of crop straw was burned, leading to high chloride emissions in this region. Lacking detailed local data may lead to this difference in RCEI\_1990 data. We validated our chloride emission inventory by comparing the simulated and observed  $\text{PM}_{2.5}\text{-Cl}^-$  concentrations at a site<sup>65</sup> in Changchun ( $43.87^\circ\text{N}$ ,  $125.28^\circ\text{E}$ ) in the Northeast China. The simulation was conducted for the period from March 5 to April 5, 2014, using a 3D chemistry transport model, the Community Multiscale Air Quality (CMAQ) Modeling System version 5.1. The model configurations were the same as those described in Fu et al.<sup>66</sup> As shown in Figure S2, the simulated  $\text{PM}_{2.5}\text{-Cl}^-$  with this new chloride emission inventory exhibited better agreement than the simulation with the RCEI\_1990 in the comparison with observations, with NMB (normalized mean biases) decreasing from  $-64.3\%$  to  $-32.7\%$  and correlation coefficient ( $R$ ) increasing from 0.25 to 0.6.

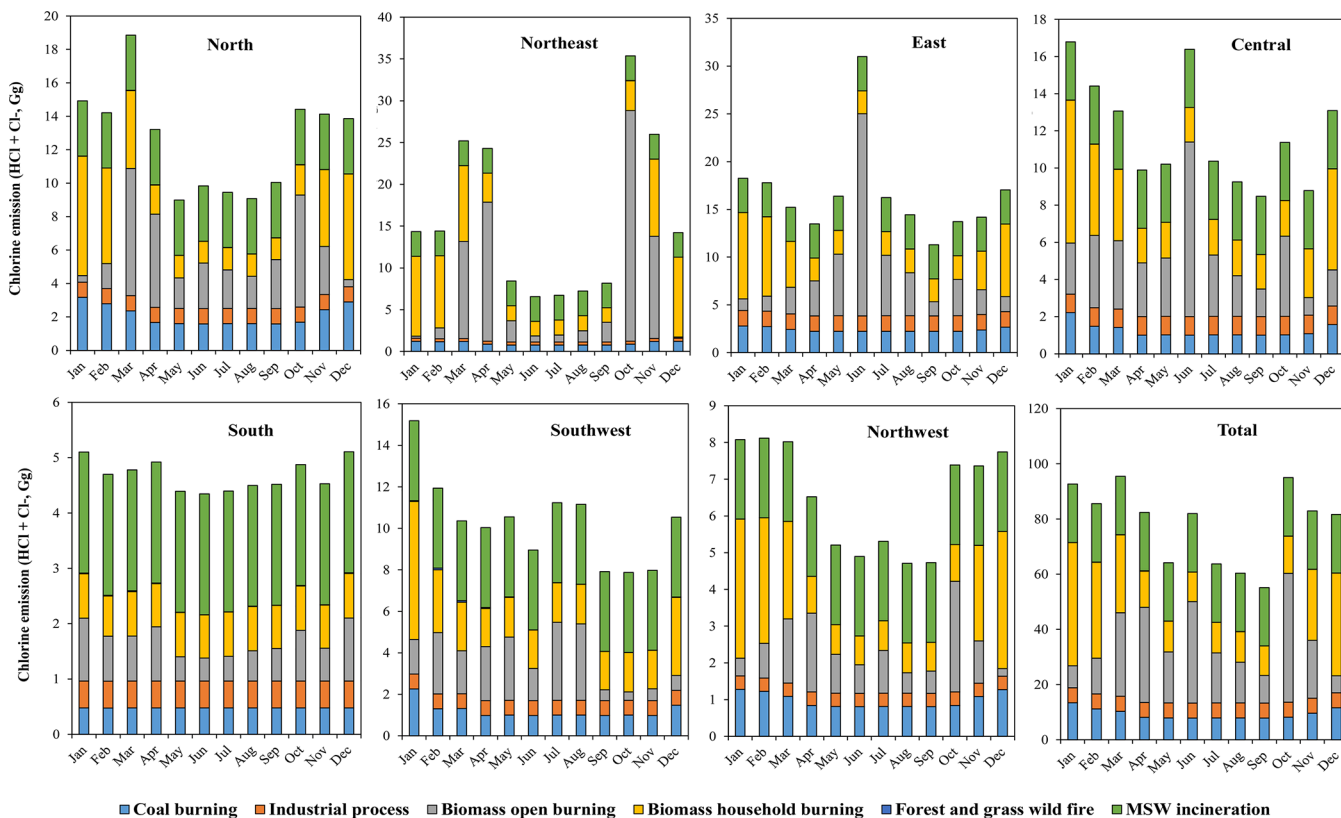


Figure 4. Monthly distribution of chlorine emission (HCl + Cl<sup>-</sup>) in different regions.

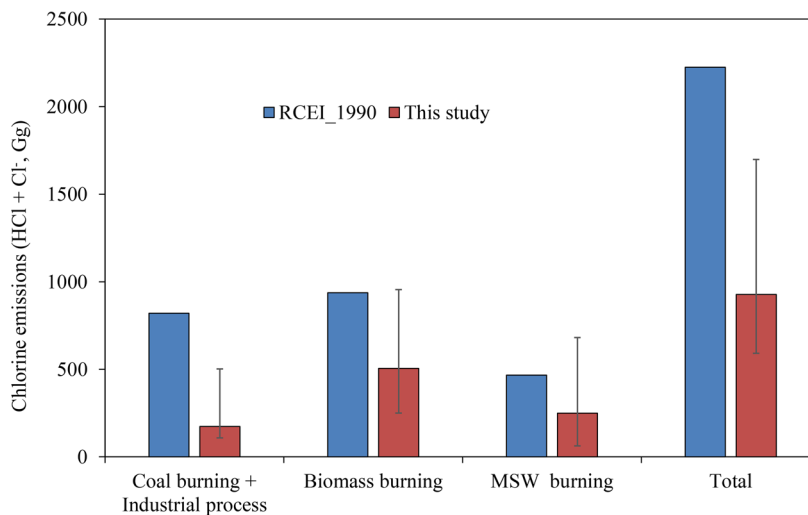


Figure 5. Comparison with RCEI\_1990. The error bars represent the uncertainties of chlorine emissions estimated in this study.

**3.5. Uncertainty Analysis.** The Monte Carlo method<sup>67,68</sup> was applied to quantify the uncertainties for this emission inventory. Normal distributions with coefficients of variation (CV) of 5%–30% were assumed for activity data.<sup>18,67</sup> For other parameters, probability distributions were fitted for parameters with adequate measurement data, e.g., Cl content in coal (Table S2). For parameters with limited measurement data, probability distributions were assumed as uniform or log-normal distributions. The detailed uncertainty assumptions are summarized in Table S4. The uncertainties for the HCl and fine particulate Cl<sup>-</sup> emissions were estimated to be -33~83% and -40~82% at a 95% confidence interval, respectively. MSW

burning and coal burning were major contributors for the uncertainties. For MSW burning, the uncertainties were -72~141% and -85~233% for the HCl and fine particulate Cl<sup>-</sup> emissions, respectively, mainly resulting from high uncertainties of emission factors for MSW open burning. The uncertainty of HCl emissions from coal burning was -32~254%, mainly resulting from high uncertainties of Cl content in coal. As shown in Table S2, the P95 values were 467%, 199%, and 694% higher than the P50 values for Cl content in coal in Inner Mongolia, Shanxi, and Shaanxi, respectively.

In order to lower the uncertainties, more local measurements are needed, e.g., for emission factors of MSW open burning, Cl content in coal from large coal producers, and the impacts of sulfur contents in coal on HCl emissions. The effects of different control technologies on Cl<sup>-</sup> percentages in PM<sub>2.5</sub> emissions need to be explored further. Additionally, the present inventory did not include the coarse particulate Cl<sup>-</sup> emissions, due to very limited testing data for Cl<sup>-</sup> percentage in coarse particle emissions. More studies are needed in the future. In order to verify further this emission inventory, we suggest to conduct HCl and particulate Cl<sup>-</sup> observations at more sites and in different seasons. In addition to chemistry transport models, source apportionment methods can be used to evaluate the sectoral contributions of this chloride emission inventory. Despite the uncertainties, the present inventory provides up-to-date and finer estimation of chloride emissions in China with detailed local data, which enables better quantification of the ClNO<sub>2</sub> production and its impact over China.

## ■ ASSOCIATED CONTENT

### 📄 Supporting Information

The Supporting Information is available free of charge on the ACS Publications website at DOI: 10.1021/acs.est.7b05030.

Emission source categorization (Table S1); key characteristics of distribution functions for Cl content in raw coal produced in major provinces in China (Table S2); Cl percentages in PM<sub>2.5</sub> emissions from different sources (Table S3); assumptions for uncertainty analysis (Table S4); spatial distribution of chlorine emission intensity in RCEI data and this study (Figure S1); comparison of observed and simulated PM<sub>2.5</sub>-Cl<sup>-</sup> concentrations at Changchun site based on the chlorine emissions from RCEI\_1990 and this study (Figure S2) (PDF)

## ■ AUTHOR INFORMATION

### Corresponding Authors

\*Tel.: +86-852-27666059. Fax: +86-852-23569054. E-mail: tao.wang@polyu.edu.hk (T.W.).

\*Tel.: +86-852-27664091. Fax: +86-852-23569054. E-mail: x.fu@polyu.edu.hk (X.F.).

### ORCID

Xiao Fu: 0000-0002-2993-0522

Shuxiao Wang: 0000-0003-3381-4767

### Notes

The authors declare no competing financial interest.

## ■ ACKNOWLEDGMENTS

This work was sponsored by the China National Natural Science Foundation (91544213), the Hong Kong Research Grants Council (C5022-14G), Hong Kong Theme-Based Research Scheme (T24-S04/17-N), and Hong Kong PolyU Project of Strategic Importance (1-ZE13).

## ■ REFERENCES

- (1) Saiz-Lopez, A.; von Glasow, R. Reactive halogen chemistry in the troposphere. *Chem. Soc. Rev.* **2012**, *41*, 6448–6472.
- (2) Finlaysonpitts, B. J.; Ezell, M. J.; Pitts, J. N. Formation of chemically active chlorine compounds by reactions of atmospheric NaCl particles with gaseous N<sub>2</sub>O<sub>5</sub> and ClNO<sub>2</sub>. *Nature* **1989**, *337*, 241–244.
- (3) Thornton, J. A.; Kercher, J. P.; Riedel, T. P.; Wagner, N. L.; Cozic, J.; Holloway, J. S.; Dube, W. P.; Wolfe, G. M.; Quinn, P. K.

Middlebrook, A. M.; Alexander, B.; Brown, S. S. A large atomic chlorine source inferred from mid-continental reactive nitrogen chemistry. *Nature* **2010**, *464*, 271–274.

- (4) Tham, Y. J.; Wang, Z.; Li, Q. Y.; Yun, H.; Wang, W. H.; Wang, X. F.; Xue, L. K.; Lu, K. D.; Ma, N.; Bohn, B.; Li, X.; Kecorius, S.; Gross, J.; Shao, M.; Wiedensohler, A.; Zhang, Y. H.; Wang, T. Significant concentrations of nitryl chloride sustained in the morning: investigations of the causes and impacts on ozone production in a polluted region of northern China. *Atmos. Chem. Phys.* **2016**, *16*, 14959–14977.

- (5) Wang, T.; Tham, Y. J.; Xue, L.; Li, Q.; Zha, Q.; Wang, Z.; Poon, S. C. N.; Dube, W. P.; Blake, D. R.; Louie, P. K. K.; Luk, C. W. Y.; Tsui, W.; Brown, S. S. Observations of nitryl chloride and modeling its source and effect on ozone in the planetary boundary layer of southern China. *J. Geophys. Res.* **2016**, *121*, 2476–2489.

- (6) Keene, W. C.; Khalil, M. A. K.; Erickson, D. J.; McCulloch, A.; Graedel, T. E.; Lobert, J. M.; Aucott, M. L.; Gong, S. L.; Harper, D. B.; Kleiman, G.; Midgley, P.; Moore, R. M.; Seuzaret, C.; Sturges, W. T.; Benkovitz, C. M.; Koropalov, V.; Barrie, L. A.; Li, Y. F. Composite global emissions of reactive chlorine from anthropogenic and natural sources: Reactive Chlorine Emissions Inventory. *J. Geophys. Res.* **1999**, *104*, 8429–8440.

- (7) National Bureau of Statistics (NBS). *China Energy Statistical Yearbook 2015*; China Statistics Press: Beijing, China, 2015.

- (8) National Bureau of Statistics (NBS). *China Statistical Yearbook 2015*; China Statistics Press: Beijing, China, 2015.

- (9) Lei, Y.; Zhang, Q. A.; Nielsen, C.; He, K. B. An inventory of primary air pollutants and CO<sub>2</sub> emissions from cement production in China, 1990–2020. *Atmos. Environ.* **2011**, *45*, 147–154.

- (10) The 13th five-year development plan of lime industry. <http://www.chinakalk.com/showexhibition.asp?id=22> (accessed September 27, 2017).

- (11) National Bureau of Statistics (NBS). *Guide to the catalogue of national key energy conservation technology promotion*; China Finance and Economics Press: Beijing, China, 2012.

- (12) National Bureau of Statistics (NBS). *Tabulation on the 2010 population census of the People's Republic of China by county*; China Statistics Press: Beijing, China, 2012.

- (13) National Bureau of Statistics (NBS). *China County Construction Statistical Yearbook 2015*; China Statistics Press: Beijing, China, 2015.

- (14) National Bureau of Statistics (NBS). *China Urban Construction Statistical Yearbook 2015*; China Statistics Press: Beijing, China, 2015.

- (15) Fu, X.; Wang, S. X.; Ran, L. M.; Pleim, J. E.; Cooter, E.; Bash, J. O.; Benson, V.; Hao, J. M. Estimating NH<sub>3</sub> emissions from agricultural fertilizer application in China using the bi-directional CMAQ model coupled to an agro-ecosystem model. *Atmos. Chem. Phys.* **2015**, *15*, 6637–6649.

- (16) Peng, L.; Zhang, Q.; He, K. Emission inventory of atmospheric pollutants from open burning of crop residues in China based on a national questionnaire. *Res. Environ. Sci.* **2016**, *29*, 1109–1118.

- (17) Zhang, G.; Lu, F.; Zhao, H.; Yang, G.; Wang, X.; Ouyang, Z. Residue usage and farmers' recognition and attitude toward residue retention in China's croplands. *J. Agro-Environ. Sci.* **2017**, *36*, 981–988.

- (18) Zhou, Y.; Xing, X. F.; Lang, J. L.; Chen, D. S.; Cheng, S. Y.; Wei, L.; Wei, X.; Liu, C. A comprehensive biomass burning emission inventory with high spatial and temporal resolution in China. *Atmos. Chem. Phys.* **2017**, *17*, 2839–2864.

- (19) National Bureau of Statistics (NBS). *China Energy Statistical Yearbook 2006–2008*; China Statistics Press: Beijing, China, 2006–2008.

- (20) Tian, Y. Current Development Situation and Trend of China's Rural Energy in 2013. *Energy of China* **2014**, *36*, 10–14.

- (21) Fang, J. Y.; Liu, G. H.; Xu, S. L. Biomass and net production of forest vegetation in China. *Acta Ecol. Sin.* **1996**, *16*, 497–508.

- (22) Pu, S. L.; Fang, J. Y.; He, J. S.; Xiao, Y. Spatial distribution of grassland biomass in China. *Zhiwu Shengtai Xuebao* **2004**, *28*, 491–498.

- (23) Hu, H. F.; Wang, Z. H.; Liu, G. H.; Fu, B. J. Vegetation carbon storage of major shrublands in China. *Zhiwu Shengtai Xuebao* **2006**, *30*, 539–544.
- (24) Intergovernmental Panel on Climate Change (IPCC). *IPCC Guidelines for National Greenhouse Gas Inventories*; National Greenhouse Gas Inventories Programme Japan: Geneva, Switzerland, 2006.
- (25) Wang, Y.; Cheng, K.; Wu, W. D.; Tian, H. Z.; Yi, P.; Zhi, G. R.; Fan, J.; Liu, S. H. Atmospheric emissions of typical toxic heavy metals from open burning of municipal solid waste in China. *Atmos. Environ.* **2017**, *152*, 6–15.
- (26) He, P.; Zhang, C.; Yang, N.; Zhang, H.; Lv, F.; Shao, L. Present Situation and Technical Treatment Route of Rural Domestic Waste Treatment in China. *J. Agro-Environ. Sci.* **2010**, *29*, 2049–2054.
- (27) Ma, Q. A.; Cai, S. Y.; Wang, S. X.; Zhao, B.; Martin, R. V.; Brauer, M.; Cohen, A.; Jiang, J. K.; Zhou, W.; Hao, J. M.; Frostad, J.; Forouzanfar, M. H.; Burnett, R. T. Impacts of coal burning on ambient PM<sub>2.5</sub> pollution in China. *Atmos. Chem. Phys.* **2017**, *17*, 4477–4491.
- (28) Wang, S. X.; Zhao, B.; Cai, S. Y.; Klimont, Z.; Nielsen, C. P.; Morikawa, T.; Woo, J. H.; Kim, Y.; Fu, X.; Xu, J. Y.; Hao, J. M.; He, K. B. Emission trends and mitigation options for air pollutants in East Asia. *Atmos. Chem. Phys.* **2014**, *14*, 6571–6603.
- (29) Zhao, B.; Wang, S. X.; Wang, J. D.; Fu, J. S.; Liu, T. H.; Xu, J. Y.; Fu, X.; Hao, J. M. Impact of national NO<sub>x</sub> and SO<sub>2</sub> control policies on particulate matter pollution in China. *Atmos. Environ.* **2013**, *77*, 453–463.
- (30) Zhang, L.; Wang, S. X.; Meng, Y.; Hao, J. M. Influence of Mercury and Chlorine Content of Coal on Mercury Emissions from Coal-Fired Power Plants in China. *Environ. Sci. Technol.* **2012**, *46*, 6385–6392.
- (31) Chen, X.; Zhou, J.; Zeng, X.; A, M.; Ge, D.; Yang, S. Characteristics and Distribution of Coal in Zhundong Coalfield. *Xinjiang Geol.* **2013**, *31*, 89–93.
- (32) Dai, S. F.; Jiang, Y. F.; Ward, C. R.; Gu, L. D.; Seredin, V. V.; Liu, H. D.; Zhou, D.; Wang, X. B.; Sun, Y. Z.; Zou, J. H.; Ren, D. Y. Mineralogical and geochemical compositions of the coal in the Guanbanwusu Mine, Inner Mongolia, China: Further evidence for the existence of an Al (Ga and REE) ore deposit in the Jungar Coalfield. *Int. J. Coal Geol.* **2012**, *98*, 10–40.
- (33) Dai, S. F.; Seredin, V. V.; Ward, C. R.; Hower, J. C.; Xing, Y. W.; Zhang, W. G.; Song, W. J.; Wang, P. P. Enrichment of U-Se-Mo-Re-V in coals preserved within marine carbonate successions: geochemical and mineralogical data from the Late Permian Guiding Coalfield, Guizhou. *Miner. Deposita* **2015**, *50*, 159–186.
- (34) Guo, G.; Yang, C.; Gong, G. Quality and utilization of the coal from Taiyuan formation and Shanxi formation in Suhaitu-Kucaowa area, Inner Mongolia. *Geol. Res.* **2017**, *26*, 34–37.
- (35) Hu, S. The study of chlorine in Huangling coal. *China Coal* **2004**, *30*, 64–67.
- (36) Jiang, X.; Xu, X.; Yan, J.; He, J.; Chi, C.; Qin, K. The distribution of chlorine in coal and the experimental study of chlorine release during combustion. *J. China Coal Soc.* **2001**, *26*, 667–670.
- (37) Li, D.; Tang, Y.; Chen, K.; Deng, T.; Cheng, F.; Liu, D. Distribution of twelve toxic trace elements in coals from Southwest China. *J. China U. Min. Techno.* **2006**, *35*, 15–20.
- (38) Liu, D. M.; Yang, Q.; Tang, D. Z.; Kang, X. D.; Huang, W. H. Geochemistry of sulfur and elements in coals from the Antaibao surface mine, Pingshuo, Shanxi Province, China. *Int. J. Coal Geol.* **2001**, *46*, 51–64.
- (39) Sun, C.; Zhang, W.; Huang, C.; Chen, B. Coal characteristics of Xishan kiln in Nileke, Xinjiang. *West-China Exploration Engineering* **2015**, *2*, 140–142.
- (40) Sun, R. Y.; Liu, G. J.; Zheng, L. G.; Chou, C. L. Characteristics of coal quality and their relationship with coal-forming environment: A case study from the Zhuji exploration area, Huainan coalfield, Anhui, China. *Energy* **2010**, *35*, 423–435.
- (41) Zhang, J.; Zhang, H.; Du, J.; Hu, C.; Pan, H.; Ding, N. Distribution characteristics of trace elements in coal of Inner Mongolia Baiyinhuo coalfield. *J. China Coal Soc.* **2016**, *41*, 310–315.
- (42) Streets, D. G.; Hao, J. M.; Wu, Y.; Jiang, J. K.; Chan, M.; Tian, H. Z.; Feng, X. B. Anthropogenic mercury emissions in China. *Atmos. Environ.* **2005**, *39*, 7789–7806.
- (43) Liu, X.; Liu, J.; Zhang, J.; Song, D.; Zheng, C. Migration and Removability of Fluorine and Chlorine from Guizhou Shuicheng Coal During Cleaning Process. *J. Power Eng.* **2009**, *29*, 970–976.
- (44) Deng, S.; Zhang, C.; Liu, Y.; Cao, Q.; Xu, Y.; Wang, H.; Zhang, F. A full-scale field study on chlorine emission of pulverized coal-fired power plants in China. *Environm.Sci.* **2014**, *27*, 127–133.
- (45) Paradiz, B.; Dilara, P.; Umlauf, G.; Bajsic, I.; Butala, V. DIOXIN EMISSIONS FROM COAL COMBUSTION IN DOMESTIC STOVE: FORMATION IN THE CHIMNEY AND COAL CHLORINE CONTENT INFLUENCE. *Therm. Sci.* **2015**, *19*, 295–304.
- (46) Cheng, C. M.; Hack, P.; Chu, P.; Chang, Y. N.; Lin, T. Y.; Ko, C. S.; Chiang, P. H.; He, C. C.; Lai, Y. M.; Pan, W. P. Partitioning of Mercury, Arsenic, Selenium, Boron, and Chloride in a Full-Scale Coal Combustion Process Equipped with Selective Catalytic Reduction, Electrostatic Precipitation, and Flue Gas Desulfurization Systems. *Energy Fuels* **2009**, *23*, 4805–4816.
- (47) Cordoba, P.; Font, O.; Izquierdo, M.; Querol, X.; Tobias, A.; Lopez-Anton, M. A.; Ochoa-Gonzalez, R.; Diaz-Somoano, M.; Martinez-Tarazona, M. R.; Ayora, C.; Leiva, C.; Fernandez, C.; Gimenez, A. Enrichment of inorganic trace pollutants in re-circulated water streams from a wet limestone flue gas desulphurisation system in two coal power plants. *Fuel Process. Technol.* **2011**, *92*, 1764–1775.
- (48) Meij, R.; Winkel, H. T. The emissions of heavy metals and persistent organic pollutants from modern coal-fired power stations. *Atmos. Environ.* **2007**, *41*, 9262–9272.
- (49) Jiang, X.; Li, X.; Chi, C.; Yan, J. Experimental study of emission of HCl on incinerating of typical MSW components and coal in fluidized bed. *Proceed. CSEE* **2004**, *24*, 213–217.
- (50) Tan, J. J.; Yang, G. H.; Mao, J. Q.; Dai, H. C. Laboratory study on high-temperature adsorption of HCl by dry-injection of Ca(OH)<sub>2</sub> in a dual-layer granular bed filter. *Front. Environ. Sci. Eng.* **2014**, *8*, 863–870.
- (51) Li, L.; Huang, Q.; Zhang, Z.; Cai, M.; Yan, D. Pollution emission of co-processing polluted soil in a cement kiln. *Chinese J. Environmental Engineering* **2009**, *3*, 891–896.
- (52) Li, Y. Q.; Zhan, M. X.; Chen, T.; Zhang, J.; Li, X. D.; Yan, J. H.; Buekens, A. Formation, Reduction and Emission Behaviors of CBzs and PCDD/Fs from Cement Plants. *Aerosol Air Qual. Res.* **2016**, *16*, 1942–1953.
- (53) Wang, B.; Jiang, Y. Technology of cement kiln co-processing city living garbage and the application state in China. *Cem. Eng.* **2014**, *4*, 74–78.
- (54) Hu, B.; Yu, S.; Gui, Y.; Mi, J.; Qin, R. Study on Chlorine Balance in Sintering Process of Tangsteel. *Sintering Pelletizing* **2013**, *38*, 11–15.
- (55) Stockwell, C. E.; Yokelson, R. J.; Kreidenweis, S. M.; Robinson, A. L.; DeMott, P. J.; Sullivan, R. C.; Reardon, J.; Ryan, K. C.; Griffith, D. W. T.; Stevens, L. Trace gas emissions from combustion of peat, crop residue, domestic biofuels, grasses, and other fuels: configuration and Fourier transform infrared (FTIR) component of the fourth Fire Lab at Missoula Experiment (FLAME-4). *Atmos. Chem. Phys.* **2014**, *14*, 9727–9754.
- (56) Stockwell, C. E.; Christian, T. J.; Goetz, J. D.; Jayarathne, T.; Bhawe, P. V.; Praveen, P. S.; Adhikari, S.; Maharjan, R.; DeCarlo, P. F.; Stone, E. A.; Saikawa, E.; Blake, D. R.; Simpson, I. J.; Yokelson, R. J.; Panday, A. K. Nepal Ambient Monitoring and Source Testing Experiment (NAMASTE): emissions of trace gases and light-absorbing carbon from wood and dung cooking fires, garbage and crop residue burning, brick kilns, and other sources. *Atmos. Chem. Phys.* **2016**, *16*, 11043–11081.
- (57) Burling, I. R.; Yokelson, R. J.; Griffith, D. W. T.; Johnson, T. J.; Veres, P.; Roberts, J. M.; Warneke, C.; Urbanski, S. P.; Reardon, J.; Weise, D. R.; Hao, W. M.; de Gouw, J. Laboratory measurements of trace gas emissions from biomass burning of fuel types from the southeastern and southwestern United States. *Atmos. Chem. Phys.* **2010**, *10*, 11115–11130.

- (58) Tian, H. Z.; Gao, J. J.; Lu, L.; Zhao, D.; Cheng, K.; Qiu, P. P. Temporal Trends and Spatial Variation Characteristics of Hazardous Air Pollutant Emission Inventory from Municipal Solid Waste Incineration in China. *Environ. Sci. Technol.* **2012**, *46*, 10364–10371.
- (59) Christian, T. J.; Yokelson, R. J.; Cardenas, B.; Molina, L. T.; Engling, G.; Hsu, S. C. Trace gas and particle emissions from domestic and industrial biofuel use and garbage burning in central Mexico. *Atmos. Chem. Phys.* **2010**, *10*, 565–584.
- (60) Wiedinmyer, C.; Yokelson, R. J.; Gullett, B. K. Global Emissions of Trace Gases, Particulate Matter, and Hazardous Air Pollutants from Open Burning of Domestic Waste. *Environ. Sci. Technol.* **2014**, *48*, 9523–9530.
- (61) U.S. Environmental Protection Agency (USEPA). *Compilation of Air Pollutant Emission Factors*; AP-42, fifth ed.; 1995.
- (62) Reff, A.; Bhawe, P. V.; Simon, H.; Pace, T. G.; Pouliot, G. A.; Mobley, J. D.; Houyoux, M. Emissions Inventory of PM<sub>2.5</sub> Trace Elements across the United States. *Environ. Sci. Technol.* **2009**, *43*, 5790–5796.
- (63) Huang, X.; Li, M. M.; Li, J. F.; Song, Y. A high-resolution emission inventory of crop burning in fields in China based on MODIS Thermal Anomalies/Fire products. *Atmos. Environ.* **2012**, *50*, 9–15.
- (64) Wang, S. X.; Xing, J.; Chatani, S.; Hao, J. M.; Klimont, Z.; Cofala, J.; Amann, M. Verification of anthropogenic emissions of China by satellite and ground observations. *Atmos. Environ.* **2011**, *45*, 6347–6358.
- (65) Wu, Y. H.; Wang, Y.; Zhu, N.; Qin, Y. Characteristics of PM<sub>2.5</sub> and its water-soluble ions in spring in Changchun, China. *Environ. Pollut. Control* **2017**, *39*, 398–400.
- (66) Fu, X.; Wang, S. X.; Chang, X.; Cai, S. Y.; Xing, J.; Hao, J. M. Modeling analysis of secondary inorganic aerosols over China: pollution characteristics, and meteorological and dust impacts. *Sci. Rep.* **2016**, *6*, 1–7.
- (67) Zhao, Y.; Nielsen, C. P.; Lei, Y.; McElroy, M. B.; Hao, J. Quantifying the uncertainties of a bottom-up emission inventory of anthropogenic atmospheric pollutants in China. *Atmos. Chem. Phys.* **2011**, *11*, 2295–2308.
- (68) Zheng, J. Y.; Zhang, L. J.; Che, W. W.; Zheng, Z. Y.; Yin, S. S. A highly resolved temporal and spatial air pollutant emission inventory for the Pearl River Delta region, China and its uncertainty assessment. *Atmos. Environ.* **2009**, *43*, 5112–5122.